Journal of Power Sources 242 (2013) 725–731

Contents lists available at SciVerse ScienceDirect

Journal of Power Sources

journal homepage: www.elsevier.com/locate/jpowsour

Hybrid polyelectrolytes based on stable sulfonated polynorbornene with higher proton conductivity and lower methanol permeability

Xiaohui He [a], Meiping Hu [a], Yiwang Chen [a,*], Defu Chen [b]

[a] Department of Chemistry, Institute of Polymers, Nanchang University, 999 Xuefu Avenue, Nanchang 330031, China
[b] School of Civil Engineering and Architecture, Nanchang University, 999 Xuefu Avenue, Nanchang 330031, China

HIGHLIGHTS

- Cross-linked membranes based sulfonated copoly(norbornene)s bearing sultone and zwitterionic silica are synthesized by sol–gel method.
- The membranes possess good stabilities, high proton conductivity up to 6.34×10^{-2} S cm^{-1} and comparable selectivity parameter.
- A maximum power density of 50.2 mW cm^{-2} is achieved for direct methanol fuel cells.

GRAPHICAL ABSTRACT

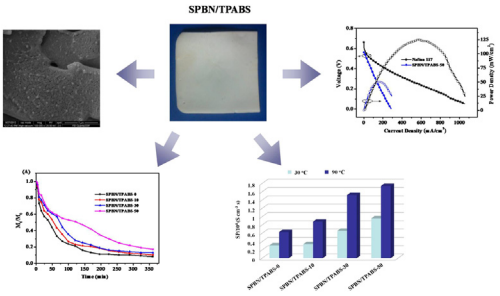

ARTICLE INFO

Article history:
Received 26 January 2013
Received in revised form
16 May 2013
Accepted 16 May 2013
Available online 6 June 2013

Keywords:
Polyelectrolytes
Fuel cells
Polynorbornenes
Sol–gel

ABSTRACT

We report preparation of hybrid cross-linked proton exchange membranes (PEMs), which are synthesized from sulfonated copoly(norbornene)s bearing sultone pendant (SPBN) and a zwitterionic silica containing sulfonic acid and ammonium groups, 3-[[3-(triethoxysilyl)-propyl]amino]butane-1-sulfonic acid (TPABS), using a sol–gel process. As these membranes are well processed as self-supporting film, they show high stabilities, proton conductivity and low methanol permeability. Reported SPBN/TPABS-50 (50 wt % of TPABS to SPBN in the matrix) shows the best performance with proton conductivity of 6.34×10^{-2} S cm^{-1}, methanol permeability of 3.64×10^{-7} cm^2 s^{-1}, ion-exchange capacity value of 1.21 mequiv g^{-1} and comparable selectivity parameter of 1.74×10^4 S cm^{-3} s. While the membrane electrode assembly (MEA) is fabricated using the SPBN/TPABS-50 as PEM, the open circuit voltage of SPBN/TPABS-50 at 1.0 M methanol (80 °C) and its power density of the devices are 0.563 V and 50.2 mW cm^{-2}, respectively, though which is lower than that of Nafion117 (124.2 mW cm^{-2}). The new designed cross-linked membranes can thus be a promising candidate to satisfy the requirements of PEMs for direct methanol fuel cells, especially the simple and low cost preparation of the membranes.

1. Introduction

A proton exchange membrane (PEM) is an essential component of the most promising electrochemical devices for convenient and efficient power generation such as polymer electrolyte membrane fuel cells (PEMFCs) and direct methanol fuel cells (DMFCs). Traditionally, DuPont's Nafion membrane has been widely extensively used in PEM materials because of its high proton conductivity and excellent stability. However, it has some drawbacks, such as high cost, high methanol permeability and limited operation temperature in fuel cells [1,2]. Many promising polymers and their composites with sulfonic acid functionality as substitutes for Nafion, such as poly(aryl ether ketone) [3], poly(ether sulfone) [4], polyimides [5], polybenzimidazole [6] etc., were studied for PEM

* Corresponding author. Tel.: +86 791 83969562; fax: +86 791 83969561.
E-mail address: ywchen@ncu.edu.cn (Y. Chen).

0378-7753/$ – see front matter © 2013 Elsevier B.V. All rights reserved.
http://dx.doi.org/10.1016/j.jpowsour.2013.05.067

applications and showed excellent stabilities and electrochemical properties. Nevertheless, sulfonation of these polymers leads to the formation of water-soluble products at high sulfonation levels and degradation of sulfonic acid groups takes place up to 240 °C [7], which is an important factor for fuel cell application.

Organic–inorganic nanostructured composites, which can overcome the drawbacks of Nafion and other membranes, have attracted much attention because they constitute a unique class of materials combining the properties of organic moieties (e.g., flexibility, dielectric, ductility, and process-ability) and the inorganic matrix (e.g., rigidity and thermal stability) and, additionally, they are synthesized through an easy processing route with low cost and less environmental impact [8–11]. In our previous work, we prepared sulfonated copoly(norbornene)s bearing sultone pendant groups (SPBN) [12] as PEM, which possessed high thermal stability, low methanol permeability, and relatively low water uptake. However, SPBN membrane showed low proton conductivity. Herein, we are reporting a method for the preparation of PEMs by dispersing organic proton-exchangers in the polymer–inorganic hybrid material synthesized by sol–gel method [13,14]. Sol–gel derived silicon oxide networks, under acid-catalyzed conditions, yield primarily linear or randomly branched polymer, which entangle and form additional branches resulting in gelation. In order to get high thermal stability, good dimensional stability and high proton conductivity, SPBN/3-[[3-(triethoxysilyl)-propyl] amino] butane-1-sulfonic acid (TPABS) blend heterogeneous PEMs were prepared by dispersing ion-exchange resin power. The inorganic nanoparticles would be stably fixed in cross-linked structure formed by ammonium and sulfonic acid interaction. In addition, the high concentrate sulfonic acid groups and organic–inorganic cross-linked structures can further make a good balance between proton conductivity and low fuel permeability. In this paper, the synthesis procedure of this new type of nanocomposite has been reported.

2. Experimental

2.1. Materials

Sulfonated copoly(norbornene)s bearing sultone pendant groups (SPBN) was prepared according to our previous procedure [12], while 3-[[3-(triethoxysilyl)-propyl]amino]butane-1-sulfonic acid (TPABS) was synthesized according to the method reported in the previous work [15]. Nafion117 (perfluorinated membrane) was provided by Aladdin Chemistry Co. Ltd and was used as received. Chlorobenzene and methanol of AR grade were purchased commercially and used without further purification. Deionized water was used for all purposes.

2.2. Membrane preparation

The membranes were prepared by two steps using a solution-casting method. A desired amount of SPBN was dissolved in chlorobenzene to obtain a 10 wt % solution under constant stirring; separately a different amount of TPABS was dissolved in chlorobenzene and mixed with an SPBN solution. Then 2.0 mL of 0.10 M HCl was added to maintain the solution pH between 2 and 3, which resulted in an acid catalyzed gel. The resulting gel was cast on a clean glass plate to the desired thickness and dried at room temperature to obtain a film. The film was dried in an oven at 50 °C for 2 h and then at 80 °C under vacuum for 24 h. Thus the membrane was peeled off and rinsed with deionized water and stored under wet conditions and cross-linked by a formal solution (HCHO + H_2SO_4) for 3 h at 60 °C. The prepared membranes were designated as SPBN/TPABS-*X*, where *X* is the weight percentage of TPABS to the SPBN (where *X* varies from 0 to 50).

2.3. Membrane characterization

2.3.1. FT IR spectroscopy

FT IR spectra of completely dried composite membranes were recorded with a Shimadzu IRPrestige-21 FT IR spectrophotometer in ATR mode. The FT IR spectrum of a synthesized TPABS was obtained by the KBr pellet method.

2.3.2. Thermal analysis

Thermal degradation and stability of the membranes were investigated using a thermo-gravimetric analyzer (TGA) (Perkin–Elmer instrument TGA 7) under a nitrogen atmosphere at a heating rate of 20 °C min^{-1} from room temperature to 600 °C.

2.3.3. Microscopic characterizations

The surface morphology of thoroughly dried membranes was studied by a JEOL JEM-2100F transmission electron microscope (TEM). The TEM samples were prepared by focused ion beam method (ion milling) and recovered on a copper grid operated at 150 kV. The surface and cross section morphology of the membranes were investigated by scanning electron microscope (SEM), using an Environmental Scanning Electron Microscope (ESEM, FEI Quanta 200). All the samples were soaked in the liquid nitrogen and fractured, followed by the sputtering of a thin layer of gold. The distribution of silica and other elements in the membrane phase was recorded by energy-dispersive X-ray (EDX) measurements carried out using a HITACHI.S-3000N Instrument.

2.3.4. Dimensional and oxidative stability

The dimensional stability was examined by immersing the square pieces of the membranes in room temperature water and 50% water–methanol for 24 h as reported previously [16], The oxidative stability was evaluated by immersing the membrane samples in Fenton's reagent (3% aqueous H_2O_2 + 3 ppm $FeSO_4$) at 80 °C for 1 h as reported in literature [16].

2.3.5. Uptake of water and ion-exchange capacity (IEC) measurements

For the measurement of water uptake, the membranes were separately immersed in deionized water and 50% water–methanol mixture for 48 h, and the wet membranes were weighed after wiping the surface with tissue paper. These wet membranes were dried at a fixed temperature of 60 °C until constant dry weight was obtained. The uptake of water was calculated using the following relationship,

$$\text{Water uptake} = \frac{W_{\text{wet}} - W_{\text{dry}}}{W_{\text{dry}}} \times 100\% \quad (1)$$

where W_{dry}, W_{wet} are the weights of dried and wet membranes, respectively.

The ion-exchange capacity is defined as the ratio between the number of exchangeable ionic groups and the weight of the dry membrane. IEC was measured by equilibrating the membrane in 0.005 M standardized NaOH solution to convert the membrane into •OH form. The membrane was then washed free of excess NaOH with deionized water and equilibrated in it to rinse the last traces of base. Then, it was equilibrated in 1.5 M NaCl solution for at least 72 h, and the ion-exchange capacity was determined from increase in basicity, which in turn was determined by acid base titration by the following equation,

$$\text{IEC} = \frac{V(\text{NaOH}) \times C(\text{NaOH})}{M(\text{membrane})} \quad (2)$$

where V(NaOH) is the volume (mL) of NaOH solution consumed, C(NaOH) is the concentration of Na^+ in the extraction solution, and M(membrane) is the dried membrane weight.

2.3.6. Membrane water retention measurements

The water retention ability of the developed membranes was evaluated by measuring water evaporation ability during the dynamic deswelling test [17]. Fully swollen membranes were placed in desiccators containing silica gel at 40 °C and were weighed after regular intervals. The weight of fully swollen membranes (W_{wet}), weight of membranes at each juncture (W_t), and dry membranes (W_{dry}) were recorded. The deswelling profile could be obtained by plotting (M_t/M_0)–time curves using the following equation [18,19],

$$\frac{M_t}{M_0} = 4\left(\frac{Dt}{\pi l^2}\right)^{1/2} \quad (3)$$

where M_0 is the initial amount of water in membrane ($M_0 = W_{wet} - W_{dry}$) and M_t is the amount of water remaining in the membrane at any given time ($M_t = W_t - W_{dry}$), D is the desorption coefficient of the water in swollen membranes, and l is the membrane thickness.

2.3.7. Membrane conductivity measurements

The proton conductivities (δ) of the SPBN/TPABS blend membranes were evaluated at different temperatures (30–90 °C) by three-electrode electrochemical impedance spectra method, using a CHI660 electrochemical workstation (CH Instruments). The sample was sandwiched between two PTFE gaskets in a PTFE diffusion cell composed of two symmetrical chambers. The cells were filled with the electrolyte composed of sulfuric acid (0.5 M). The two platinum wires using as working electrode and counter electrode, as well as a Ag/AgCl electrode functionalized as the reference electrode were introduced into the electrolyte solution. The impedance spectra were recorded with the help of ZPlot/ZView software under an ac perturbation signal of 10 mV over the frequency range of 0.1 MHz–1 Hz. The electron resistant of the system (without membrane divided) was measured as R_1, and the electron resistant of the system (with membrane divided) was measured as R_2. The proton conductivity (δ) of the membrane was calculated from the following equation:

$$\delta = L/(RA) \quad (4)$$

where δ, L, R, and A represent the proton conductivity, thickness of membranes, the resistance of the membrane and the cross-sectional area of the membrane, respectively.

2.3.8. Methanol permeability measurements

An organic glass diffusion cell was used to obtain the methanol permeability of the membranes. The diffusion cell was composed of two membrane sample. One chamber of the cell (V_1) was filled with a 5 M (C_1) methanol solution in distilled water. The other chamber (V_2) was filled with water. A sample (effective area 0.385 cm^2) was clamped between the two chambers. Methanol permeates across the membrane by the concentration difference between the two chambers. The methanol concentration in the receiving chamber as a function of time is given by:

$$C_2(t) = [ADKC_1(t - t_0)]/(V_2 l) \quad (5)$$

where A (cm^2) is the membrane area, l (cm) is the membrane thickness, D is the methanol diffusivity, and K is the partition coefficient between the membrane and the adjacent solution. The product DK means the membrane permeability (P):

$$P = (C_2(t)V_2 l)/[AC_1(t - t_0)] \quad (6)$$

C_2 is measured several times during the permeation experiment and the methanol permeability is obtained from the slope of the straight line. The methanol concentration was measured by using a gas chromatography of Agilent GC 6820 equipped with a FID detector.

2.3.9. Membrane electrode assembly fabrication and DMFC single cell performance test

Nafion117 and SPBN/TPABS-50 membrane performances were evaluated in a commercial fuel cell test system (Arbin BT2000) at 80 °C. The membrane electrode assembly (MEA) was prepared by the following procedures. The Pt/Ru catalyst loading of the anode was 4 mg cm^{-2}, and the Pt catalyst loading of the cathode was 3 mg cm^{-2} (Both of the electrodes were purchased from Unisizetech Company). Then, a membrane was sandwiched between anode and cathode with effective area 6.25 cm^2 by hot-pressed for 3 min under pressure of 80 kg cm^{-2} to form a MEA. For an Active mode DMFC performance test, 1.0 M methanol was supplied to anode by 3.0 mL min^{-1} flow rate, and air was supplied to cathode at the rate of 400 mL min^{-1}. After activation for several hours, the polarization curve was obtained at 80 °C [20].

3. Results and discussion

3.1. Membrane preparation

Membrane forming material was prepared by condensation polymerization of the silica precursor (3-[[3-(triethoxysilyl)-propyl]amino]butane-1-sulfonic acid) in chlorobenzene in the presence of SPBN (17.4 mol% incorporation rate of sulfonic acid moiety) with acid catalyst at room temperature for 24 h. The resulting membranes were cross-linked with formaldehyde. The representative reaction scheme is presented in Scheme 1.

3.2. FTIR spectroscopy

The ATR FT-IR spectra of the representative membranes (SPBN/TPABS-10, SPBN/TPABS-50) are recorded and given in Fig. 1. The peaks in the range of 1150–1020 cm^{-1} associated to Si–O–Si asymmetric stretching indicate the cross-linked network has successfully formed at molecular level. The intensity of the peaks varied with the content of silica precursor (TPABS) in the membrane matrix [15]. Apparently, there is no doubt that Si–O–Si groups are the results of condensation reaction between hydrolyzed silanol (Si–OH) groups, which will be in favor of better compatibility and homogeneity among organic and inorganic parts leads to a good thermal and mechanical stable membrane.

3.3. Thermal stability

Fig. 2 represents the TGA curves for SPBN/TPABS-X membranes. All thermograms (except for SPBN/TPABS-0) showed three steps weight loss: water loss (loose & bound water) from membrane phase (step I, from 30 to 150 °C), loss of sulfonic acid groups and decomposition of the polynorbornene main chain (step II, from 250 to 400 °C), and loss of quaternary ammonium group followed by membrane matrix degradation (step III, from 400 to 650 °C) hydrophilic functional groups. Rate of water loss from the membrane reduced with the increase in TPABS content, thus increase in silica content and hydrophilic functional groups. In the step III region, compare to uncross-linked SPBN/TPABS-0 membrane, the cross-linked membranes exhibited slow decomposition rate, especially for SPBN/TPABS-50, ascribing to extra quaternary ammonium

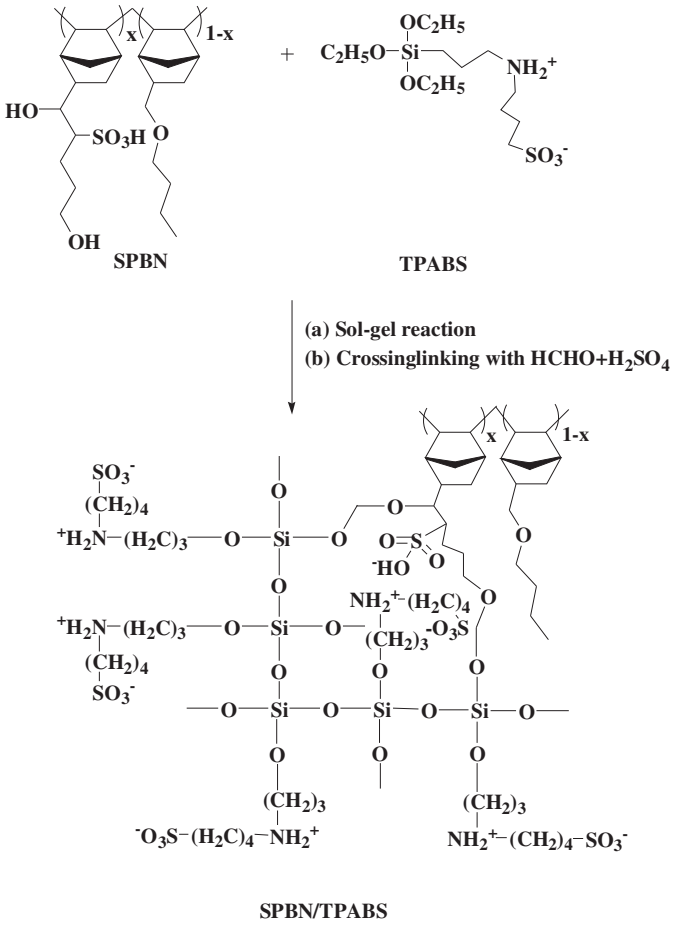

Scheme 1. Schematic route for the preparation of organic–inorganic nanocomposite membrane.

group from TPABS [21]. Based on these observations, we can conclude that functionalization at inorganic part (silica) improved thermal stabilities of the membranes and enhanced cross-linking, thus provides better stabilities.

3.4. Microscopic characterizations

Fig. 3 presents photograph, SEM (surface and cross section), EDX and TEM measurements of dry SPBN/TPABS-50 hybrid membrane (as a representative case). As shown in Fig. 3A, the SPBN/TPABS-50

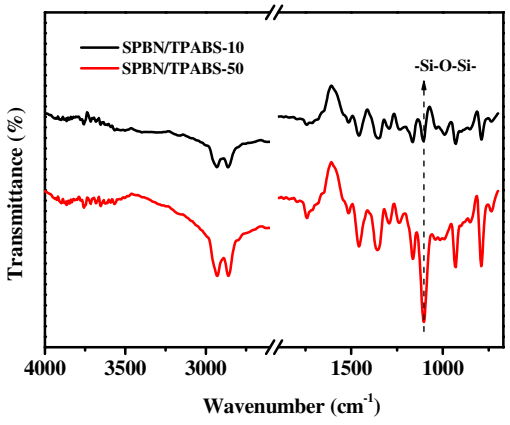

Fig. 1. FT IR spectra of the referenced cross-linked sulfonated poly(norbornene)s.

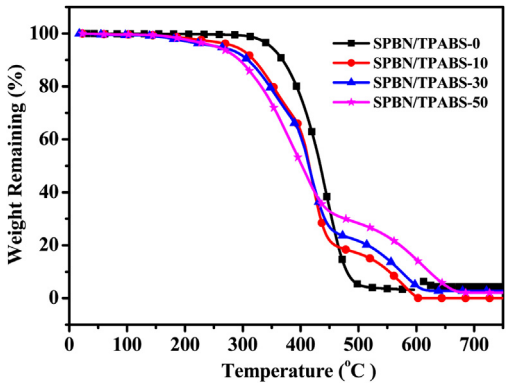

Fig. 2. TGA curves of SPBN/TPABS-*X* nanocomposite membranes.

membrane was ivory. In Fig. 3B and C showed aggregates on the membrane surface because of accelerated hydrolysis of silane and its cross-linking with SPBN. In spite of some aggregation, there was no evidence of phase separation; the cracks and holes on the membrane surface indicated the dense nature of the membrane. The control drying condition during casting is very important to avoid defects. The EDX image (Fig. 3D) confirmed the elements of the SPBN/TPABS-50 membrane and showed the presence of inorganic and organic constituents in the membrane matrix. The presence of Si, S and N would show that the TPABS was stable in the membrane matrix [18]. These results provide evidence that a well-defined, cross-linked composite membrane have been successfully prepared by SPBN and zwitterionic silica precursor via sol–gel technique. TEM was also used for microscopic characterization of the membrane, and the image is presented in Fig. 3E. This provides evidence that these hybrid membranes have nanosized silica particles homogeneously distributed within the polymer matrix. The main advantage of preparing hybrid membrane by the sol–gel method is uniform homogeneous distribution. These results suggest uniform hybrid membrane with nanosized silica and sulfonic acid clusters in the membrane phase.

3.5. Oxidative stability

Membrane stabilities and durability are important parameter to evaluate their suitability for fuel cell application. During the operation, formation of H_2O_2, •OH, and •OOH radicals, are believed to attack on hydrogen containing bonds in PEM. Weight loss of the composite membranes was tested in Fenton's reagent (3 ppm $FeSO_4$ + 3% H_2O_2) for 1 h at 80 °C, which is increased with TPABS content, and the results are revealed as oxidative weight loss percentage (W_{Ox}) in Table 1. Incorporation of TPABS, leads to increase in hydrophilic groups (contained hydrogen), which was readily attacked by peroxy radicals. About 2–6 wt % oxidative weight loss for these membranes was observed, which is similar to Nafion membrane [22]. Polynorbornene backbone and cross-linked structure may also contribute to excellent oxidative stabilities of these membranes.

3.6. Solvent uptake, dimensional changes, and water retention ability

A high water content in the membrane phase leads to deterioration in the thermal, mechanical, and chemical stabilities and H^+ concentration. Water uptake (λ_W) values of the composite membranes increased with the TBABS silica content (Table 1), may be because of the enhanced hydrophilic nature of the membrane

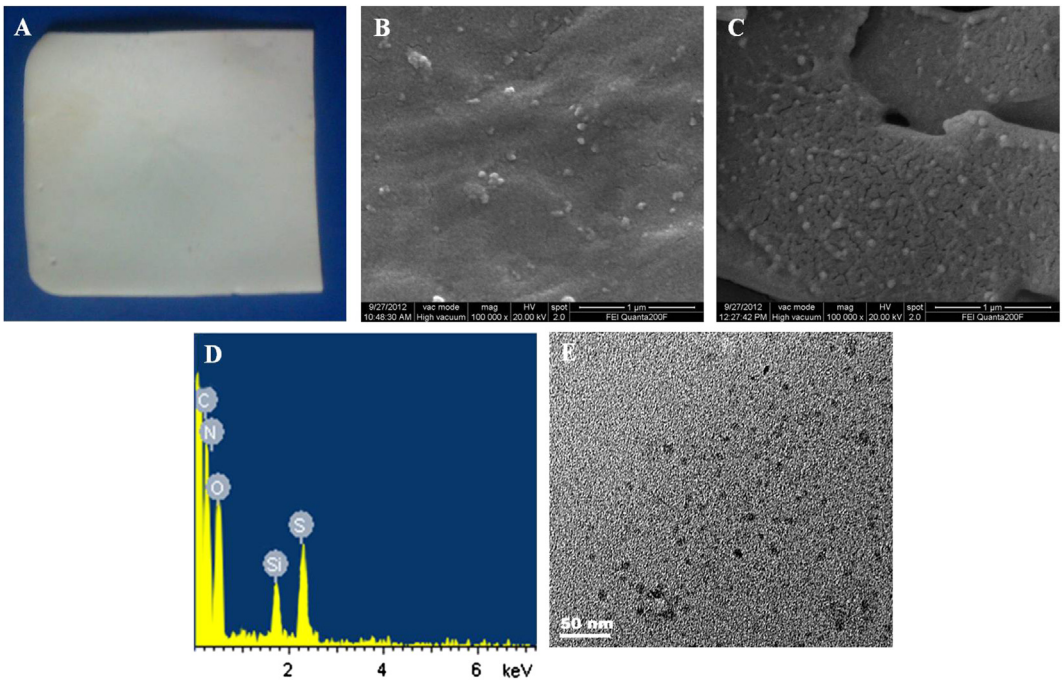

Fig. 3. Surface morphology (A) Photograph; (B) SEM (surface view); (C) SEM (cross section); (D) EDX; (E) TEM for SPBN/TPABS-50 hybrid membrane.

matrix. The solvent uptake (λ_{W+MeOH}) was also studied in a 50% water–methanol mixture to assess their suitability in DMFC, and the data are included in the same table. It is observed that the λ_{W+MeOH} values are lower than the λ_W values, suggesting that the moderate water/methanol solvent uptakes could maintain good dimensional stability of the cross-linked membranes in practical application.

Uptake water vapor sorption and desorption properties of PEMs are very important for DMFC applicability and have significant effects on the proton conductivity. The water retention capability of cross-linked membranes was illustrated in Fig. 4A ((M_t/M_0)–t (time) curves). The water retention capability dramatically improved with the degree of cross-linking and the content of TPABS increasing. Water desorption kinetics of the developed membranes was further evaluated by plotting (M_t/M_0–$t^{1/2}$) curves as a function of time in Fig. 4B using Equation (7), and calculating the desorption coefficient of the water (D) derived from Higuchi's model [17].

$$\frac{M_t}{M_0} = -kt^{1/2} + 1 \tag{7}$$

where M_0 and M_t are the initial amount of water and water remaining in polymer matrix at any given time, and k is a constant.

The obtained straight lines for varying TPABS silica content was fitted to Higuchi's model, and indicated a diffusion-controlled water desorption mechanism. Rate of water desorption was decreased with the increase of TPABS content. TPABS acted as a binder for water in the SPBN/TPABS-X matrix due to the formation of hydrophilic ionic channels and siloxane cages. Moreover, the cross-linking of the membrane has a profound effect on the water desorption property, and with the increase in cross-linking density, retention of water was increased. The water desorption coefficient

Table 1
Water uptake (λ_W), water–methanol uptake (λ_{W+MeOH}), oxidative weight loss (W_{Ox}), and water desorption coefficient (D) values for different membranes.

Membrane	λ_W wt %	λ_{W+MeOH} wt %	W_{Ox} wt %	D 10^{-6} cm^2 s
SPBN/TPABS-0	18.63	15.16	2.53	1.56
SPBN/TPABS-10	20.06	18.53	3.21	1.48
SPBN/TPABS-30	25.21	21.27	4.79	1.36
SPBN/TPABS-50	32.64	25.46	6.11	1.15

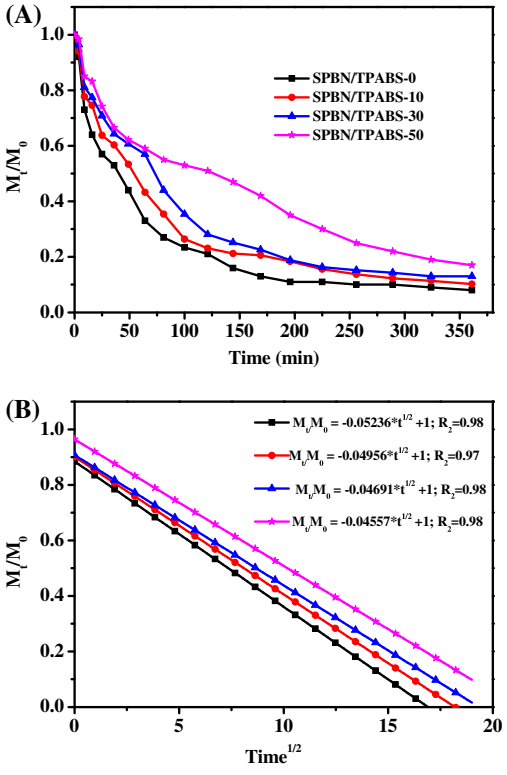

Fig. 4. Water desorption profile for SPBN/TPABS-X membranes: (A) isotherm at 40 °C; (B) Higuchi's model fit of the deswelling behavior.

Table 2
Ion-exchange capacity (IEC), proton conductivity (δ), methanol permeability (P), activation energy (E_a), and selectivity parameter (SP) values for different membrane.

Membrane	IEC mequiv g^{-1}	δ 10^{-2} S cm^{-1}	P 10^{-6} cm^2 s^{-1}	E_a KJ mol^{-1}	SP 10^4 S cm^{-3}	
					30 °C	90 °C
SPBN/TPABS-0	0.74	0.784	1.24	13.4	0.31	0.63
SPBN/TPABS-10	0.92	1.57	1.78	13.0	0.34	0.88
SPBN/TPABS-30	1.07	3.59	2.36	11.1	0.66	1.52
SPBN/TPABS-50	1.21	6.34	3.64	9.93	0.96	1.74

of water was investigated using a best-fit normalized mass change method and depicted in Table 1. Water desorption coefficient values (D) showed the similar tendency to the water retention capability of various membranes. Thus, both of TPABS and cross-linking density acted as a barrier to hinder water release and enhance water retention capacity even at higher temperature.

3.7. Ion-exchange capacity

The ion-exchange capacity indicates the density of ionizable hydrophilic functional groups, which are responsible for the proton transport. The IEC values of prepared composite membranes are tabulated in Table 2. IEC values for SPBN/TPABS membranes ranged from 0.74 mequiv g^{-1}–1.21 mequiv g^{-1}, and increased with increasing of TPABS content in membrane matrix, while Nafion117 showed a lower (0.90 mequiv g^{-1}) value [10]. IEC arose due to the presence of sulfonated acid groups and quaternary ammonium groups in the system.

3.8. Proton conductivity

For the PEMs, the proton conductivity of the membrane is particularly important since it has significant role in their fuel cell performance. Proton conductivity (δ) data for different composite membranes are also presented in Table 2. It can be seen that δ values increased with the TPABS content increasing in the membrane matrix. The SPBN/TPABS-50 showed the highest proton conductivity of 6.34×10^{-2} S cm^{-1}, at the same order of magnitude to Nafion117 (9.56×10^{-2} S cm^{-1}) [10]. More sulfonic acid groups that facilitated to transport protons or moderate water retention ability resulting from the cross-linked structure may be two of the reasons for the observed variations in proton conductivity values. The temperature dependence of proton conductivity of the fabricated membranes is shown in Fig. 5. Delightfully, in contrast with the pristine SPBN/TPABS-0, by introducing the TPABS into the polymer matrix, proton conductivity increased linearly with increasing of temperatures in the membranes. Elevated temperatures favor the dynamics of proton transport and the excellent water retention ability maintains the increased proton conductivity at high temperatures.

Proton conductivity across the composite membranes at higher temperature was also measured and results are presented as Arrhenius plots in Fig. 6. From the δ data at high temperature, energy of activation (E_a) can be estimated using following expression [23]:

$$E_a = -b \times R \tag{8}$$

where b is the slope of the regression line of ln δ (S cm^{-1}) vs. 1000/T (K^{-1}) plots and R is the gas constant (8.314 J K^{-1} mol^{-1}). The apparent activation energy (E_a) for proton conduction were determined from the slope of the Arrhenius plot and ranged between 13.4 and 9.93 kJ mol^{-1} (Table 2). E_a values decreased significantly with the TPABS content increasing in the membrane matrix. For membranes, E_a values were only slightly higher in comparison with Nafion117 membrane (6.52 kJ mol^{-1}) [15], therefore, the results of the membranes are revealed positive temperature-conductivity dependencies.

3.9. Methanol permeability and selectivity parameters studies

The methanol permeability profiles for all SPBN/TPABS membranes were determined using Equation (6), and the relevant data obtained are presented in Table 2. Methanol permeability coefficients for these SPBN/TPABS membranes (1.24–3.64 $\times$ 10^{-6} cm^2 s^{-1}) were the same order of magnitude in comparison with Nafion117 (1.310×10^{-6} cm^2 s^{-1}) [18]. The permeation of liquid molecules across polymer membrane happened via the diffusion mechanism, and the permeability of penetrate (methanol is one of the case) is the product of its solubility and diffusivity [24]. The cross-linked structures hindered the methanol to penetrate

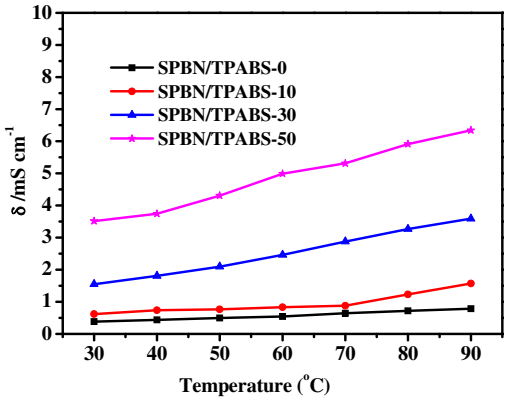

Fig. 5. Proton conductivity of the prepared membranes at different temperatures.

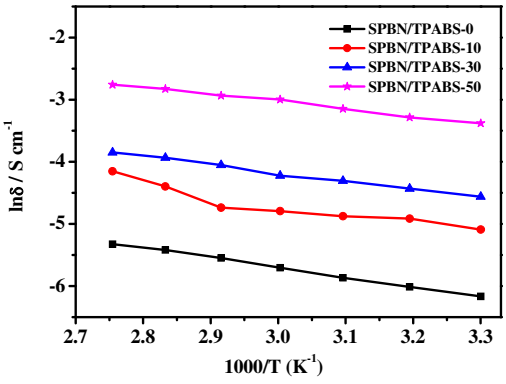

Fig. 6. Arrhenius plot for proton conductivity of different nanocomposite membranes.

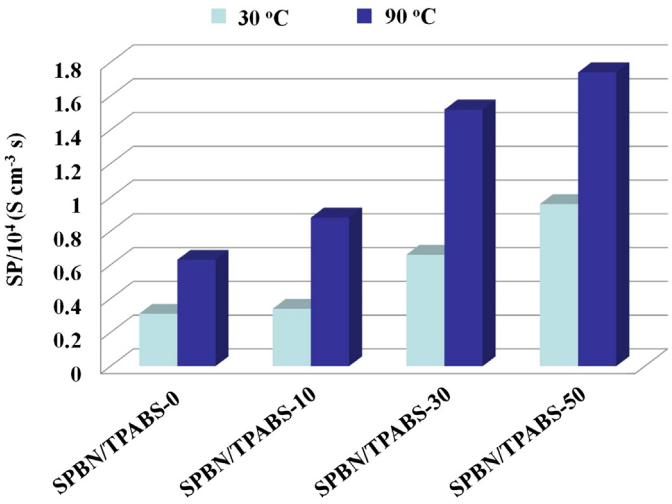

Fig. 7. Selectivity parameter values for different membranes at 30 and 90 °C.

into the membranes, because of the narrow free void volume. The methanol permeability was also increased with the TPABS content increasing due to the pronounced hydrophilicity.

To directly compare the applicability of nanocomposite SPBN/TPABS membranes for DMFC application, ratio of proton conductivity and methanol permeability (δ/P) data were used as selectivity parameter (SP) and are presented in Fig. 7. At 30 °C, SPBN/TPABS-50 membrane showed 0.96 × 10^4 S cm^{-3} s SP values, while SP for Nafion117 was 7.2 × 10^4 S cm^{-3} s in the same order of magnitude [10]. It was also observed that at 90 °C, SPBN/TPABS-50 exhibited high SP value (1.74 × 10^4 S cm^{-3} s). Increase in SP for DMFC operation at high temperature may be attributed to high proton conductivity and relatively low methanol permeability. The SP values increased with the silica content increasing, and reached a maximum when the TPABS content was 50% to SPBN in the membrane matrix. Therefore, a better understanding of the relationship between polymer structure and membrane performance, in terms of permeability and selectivity, enables us to tailor the membrane structure for specific purposes.

3.10. DMFC single cell performance

In order to test the SPBN/TPABS PEMs developed in this study in an actual DMFC, an MEA was fabricated using SPBN/TPABS-50. For comparison, an MEA with Nafion117 was also fabricated. Fig. 8 shows the preliminary results of polarization curves and power density curves at 80 °C. It was observed that SPBN/TPABS-50 PEM exhibited the open circuit voltage of 0.563 V and the maximum power density of 50.2 mW cm^{-2} which is lower than that of Nafion117 (124.2 mW cm^{-2}). This could be ascribed to the lower proton conductivity and the expedite proton transport pathway non-involved in the composite SPBN/TPABS-50 PEM [25].

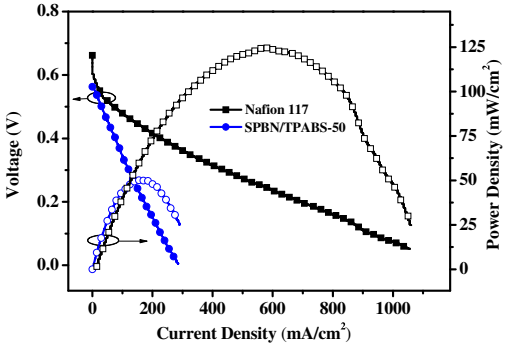

Fig. 8. DMFC single cell performances of the membranes at 80 °C.

4. Conclusions

A simple and ecofriendly procedure of nanocomposite, hybrid cross-linked membranes synthesized with SPBN and zwitterionic silica precursor TPABS by acid-catalyzed sol–gel process in chlorobenzene had been reported. The cross-linked membranes structure was confirmed by FT IR spectroscopic technique, and a schematic structure is also presented. Developed membranes showed good stabilities and water retention capacities. It was noted that the TPABS content in the membrane matrix improved the thermal stability of SPBN/TPABS membranes. The high concentrate sulfonic acid groups and organic–inorganic cross-linked structures have made a good balance between proton conductivity and low methanol permeability. MEA fabrication and active mode DMFC performance tests were carried out using SPBN/TPABS-50PEMs, and the maximum power density of 50.2 mW cm^{-2} was obtained at 80 °C. Observed proton conductivities (0.784–6.34 × 10^{-2} S cm^{-1}) of SPBN/TPABS membrane at ambient temperature and dramatically increased at higher temperature, in comparison to Nafion117 membrane, due to the activated thermal conduction process. This is a great advantage for these nanocomposite membranes to target high temperature applications.

Acknowledgments

This work was supported by the National Natural Science Foundation of China (21164006).

References

[1] B.C.H. Steele, A. Heinzel, Nature 414 (2001) 345–352.
[2] K.A. Mauritz, R.B. Moore, Chem. Rev. 104 (2004) 4535–4585.
[3] D.S. Kim, G.P. Robertson, Y.S. Kim, M.D. Guiver, Macromolecules 42 (2009) 957–963.
[4] L. Wang, B.L. Yi, H.M. Zhang, D.M. Xing, J. Phys. Chem. B 112 (2008) 4270–4275.
[5] T. Tamura, H. Kawakami, Nano Lett. 10 (2010) 1324–1328.
[6] J. Li, X. Li, Y. Zhao, W. Lu, Z. Shao, B. Yi, ChemSusChem 5 (2012) 896–900.
[7] O. Savadogo, J. Power Sources 127 (2004) 135–161.
[8] V.V. Binsu, R.K. Nagarale, V.K. Shahi, J. Mater. Chem. 15 (2005) 4823–4831.
[9] R.K. Nagarale, G.S. Gohil, V.K. Shahi, R. Rangarajan, Macromolecules 37 (2004) 10023–10030.
[10] B.P. Tripathi, V.K. Shahi, J. Phys. Chem. B 112 (2008) 15678–15690.
[11] L. Du, X. Yan, G. He, X. Wu, Z. Hu, Y. Wang, Int. J. Hydrogen Energy 37 (2012) 11853–11861.
[12] M. Hu, X. He, Y. Chen, D. Chen, J. Polym. Res. 19 (2012) 9977.
[13] L.L. Hench, J.K. West, Chem. Rev. 90 (1990) 33–72.
[14] K. Kurumada, H. Nakabayashi, T. Murataki, M. Tanigali, Colloids Surf. A 139 (1998) 163–170.
[15] L. Chen, L. Sun, R. Zeng, S. Xiao, Y. Chen, J. Power Sources 212 (2012) 13–21.
[16] B.P. Tripathi, A. Saxena, V.K. Shahi, J. Membr. Sci. 318 (2008) 288–297.
[17] T.-Y. Liu, S.-Y. Chen, Y.-L. Lin, D.-M. Liu, Langmuir 22 (2006) 9740–9745.
[18] B.P. Tripathi, V.K. Shahi, ACS Appl. Mater. Interfaces 1 (2009) 1002–1012.
[19] C. Zhao, Z. Wang, D. Bi, H. Lin, K. Shao, T. Fu, S. Zhong, H. Na, Polymer 48 (2007) 3090–3097.
[20] S. Kim, H. Lee, D. Ahn, H. Woong Park, T. Chang, W. Lee, J. Membr. Sci. 427 (2013) 85–91.
[21] Y. Xiong, Q.L. Liu, Q.G. Zhang, A.M. Zhu, J. Power Sources 183 (2008) 447–453.
[22] L. Barbora, S. Acharya, R. Singh, K. Scott, A. Verma, J. Membr. Sci. 326 (2009) 721–726.
[23] M.K. Ravikumar, A.K. Shukla, J. Electrochem. Soc. 143 (1996) 2601–2606.
[24] B.P. Ladewig, R.B. Knott, A.J. Hill, J.D. Riches, J.W. White, D.J. Martin, J.C. Diniz da Costa, G.Q. Lu, Chem. Mater. 19 (2007) 2372–2381.
[25] W. Liu, S. Wang, M. Xiao, D. Han, Y. Meng, Chem. Commun. (Cambridge, U. K.) 48 (2012) 3415–3417.